Persistence of a Two-Dimensional Topological Insulator State in Wide HgTe Quantum Wells

E. B. Olshanetsky,[1] Z. D. Kvon,[1,2] G. M. Gusev,[3] A. D. Levin,[3] O. E. Raichev,[4] N. N. Mikhailov,[1] and S. A. Dvoretsky[1]

[1]*Institute of Semiconductor Physics, Novosibirsk 630090, Russia*

[2]*Novosibirsk State University, Novosibirsk 630090, Russia*

[3]*Instituto de Física da Universidade de São Paulo, 135960-170 São Paulo, São Paulo, Brazil*

[4]*Institute of Semiconductor Physics, NAS of Ukraine, Prospekt Nauki 41, 03028 Kyiv, Ukraine*

(Received 29 August 2014; revised manuscript received 26 November 2014; published 24 March 2015)

Our experimental studies of electron transport in wide (14 nm) HgTe quantum wells confirm the persistence of a two-dimensional topological insulator state reported previously for narrower wells, where it was justified theoretically. Comparison of local and nonlocal resistance measurements indicate edge state transport in the samples of about 1 mm size at temperatures below 1 K. Temperature dependence of the resistances suggests an insulating gap of the order of a few meV. In samples with sizes smaller than 10 μm a quasiballistic transport via the edge states is observed.

DOI: 10.1103/PhysRevLett.114.126802 PACS numbers: 73.43.Fj, 73.23.-b, 85.75.-d

Topological insulators (TI) represent a quantum state of condensed matter with insulating bulk and conducting gapless states at the surface or edge [1–4]. The existence of such materials is justified within a concept of topological ordering introducing order parameters which are often expressed as invariant integrals over the momentum space. In the presence of time reversal symmetry, the materials with energy band gaps (band insulators) are classified by Z_2 topological invariants [5] that take two values, 1 or 0, thereby providing a distinction between topological and normal insulators. Mathematically, one can construct Z_2 invariants in different ways, but their physical meaning always relies on the symmetry of electron wave function, which is changed as a result of energy band inversion. Such an inversion occurs due to spin-orbit coupling and Darwin term contributions in the Hamiltonians of the crystals formed from heavy atoms. There are three types of band inversions (s-p, p-p, and d-f) in the three-dimensional (3D) TI discovered so far [6].

The most extensively studied TI materials, bismuth chalcogenides and related alloys, belong to the p-p inversion type. For thin layers of these materials, one expects a dimensionality crossover: when layer thickness d decreases, the material transforms from 3D TI into two-dimensional (2D) TI [7]. This occurs when the wave function decay length of the surface states becomes comparable to d. As a result, the 2D states from opposite surfaces hybridize and their spectrum is no longer gapless [7,8]. On the other hand, since the surface states in TI cover the whole surface of the layer, including side regions, they are transformed into 1D conducting edge channels in these regions, Fig. 1(a) [9].

A special place in this connection belongs to HgTe, a zinc blende-structure crystal with s-p band inversion, where the energy of a p-type Γ_8 band in the Γ point of the Brillouin zone is higher than the energy of an s-type Γ_6 band. In spite of the inversion, bulk HgTe is not a 3D TI because it is a symmetry-protected gapless material. A gap can be opened in a thin HgTe layer sandwiched between $Cd_{1-x}Hg_xTe$ layers (normal insulators), as realized in epitaxially grown quantum wells (QWs). Becuase of size quantization, the heavy-hole (hh) continuum that forms the valence band in HgTe splits into a set of 2D states hybridized with two interfacelike states S1 and S2, Fig. 1(b). The gap between the ground-state hh subband (hh1) and the next adjacent subband exists for QW narrower than 18 nm (for wider wells the QW is in a semimetallic state). Since the gap opening is accompanied with the dimensionality crossover, a HgTe-based QW should be a 2D TI having edge states in the gap between subbands. However, a direct theoretical proof for this statement, based on a two-subband effective 2D Hamiltonian [18], has been done only for a special situation when the S1 subband is just slightly below the hh1 subband, which is applicable to narrow wells in the width range of approximately 6.3–7.3 nm. The edge state transport in such QWs was also confirmed experimentally [19]. In wider HgTe QWs, any effective Hamiltonian methods are not generally feasible because of a complicated subband structure, though a usage of the three-subband (S1, hh1, and hh2) basis [20] extends the range of applicability of such methods. In particular, it was found that when the S1 subband falls below hh2 one (so the principal gap is formed between the hh1 and hh2 subbands), the edge states exist both in this gap and in the next gap between the hh2 and S1 subbands.

A question that naturally arises concerns the persistence of the 2D TI state in wide QWs where the S1 subband lies

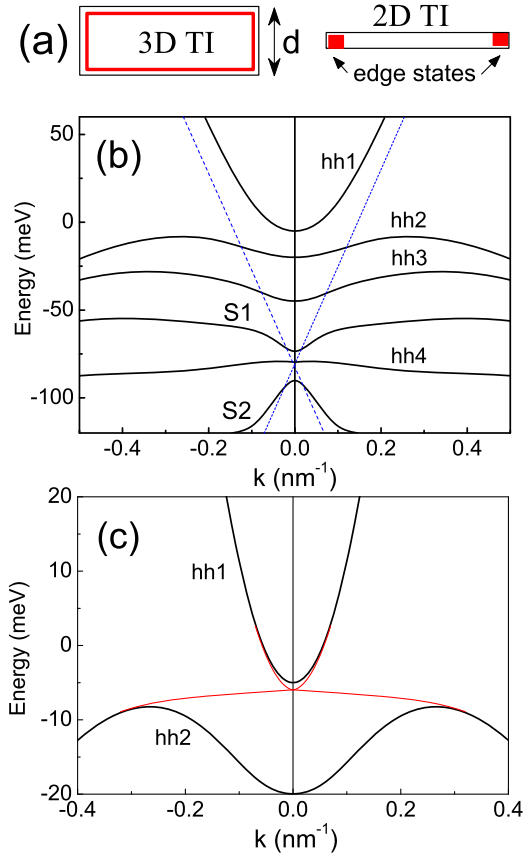

FIG. 1 (color online). (a) Cross section of a 3D TI sample (schematic) with surface state channels shown in red. As the thickness of the sample decreases, a transition to 2D TI takes place. (b) Energy spectrum of size-quantized subbands in a symmetric 14 nm wide $Cd_{0.65}Hg_{0.35}Te/HgTe/Cd_{0.65}Hg_{0.35}Te$ QW, calculated numerically by using Kane Hamiltonian (the Kane model parameters are presented in the Supplemental Material [10]). Dashed (blue) lines show the spectrum of interface states at a single $HgTe/Cd_{0.65}Hg_{0.35}Te$ boundary under approximation that mixing of these states with hh states is neglected. (c) A magnified picture of two upper hh subbands and the expected edge state spectrum, thin (red) lines, in the gap between them.

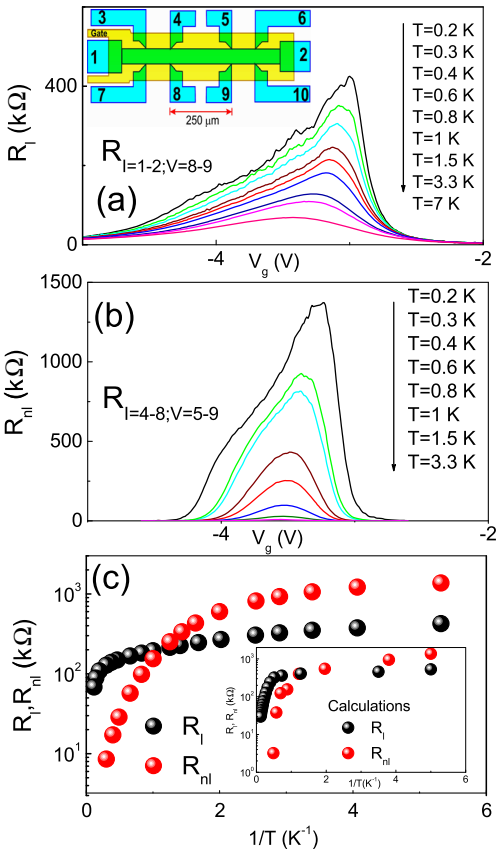

FIG. 2 (color online). Local (a) and nonlocal (b) resistance at different temperatures, sample I, $B = 0$ (the inset shows a schematic view of the sample). (c) Temperature dependence of local and nonlocal resistance when the Fermi energy is situated in the center of the insulating bulk gap (the inset shows calculations).

below several hh subbands, so the situation is far different from that described theoretically in Refs. [18] and [20]. From the point of view of dimensionality crossover, there is no reason to deny the 2D TI nature of these systems, since widening of the QW (actually, approaching of the HgTe layer to the bulk state) does not cancel the fact of s-p inversion in this layer and, accordingly, cannot destroy the edge states. In this Letter we report experimental investigation of 14 nm wide HgTe QWs, which are wider than those studied previously [19,21,22] but still have a sizeable gap of a few meV between the hh1 and hh2 subbands. We plot the expected edge states in this gap schematically in Fig. 1(c) as two (one for each spin number) gapless branches merging with 2D subbands on a tangent. By transport measurements, we indeed obtain numerous proofs for the edge state transport in these QWs.

The experimental samples are Hall bridges fabricated on top of the 14 nm wide HgTe QW with the surface orientation (112) and provided with an electrostatic gate. Their fabrication technology is described in detail in [23]. Three different types of experimental samples were used: macroscopic Hall bridges (see Fig. 2) with the width 50 μm and the distance between the voltage probes 100 and 250 μm, and two types of microscopic samples, whose layout together with the scale is shown in Fig. 3 [10]. The transport measurements were conducted in the temperature range 0.2–10 K and in magnetic fields up to 10 T using the standard phase detecting scheme on frequencies 3–12 Hz and the driving current 0.1–1 nA to avoid heating effects. The electron mobility μ in all samples studied was above 10^5 cm^2/V s for the carrier density 3×10^{11} cm^{-2}.

We first consider the properties of our macroscopic samples. Observation of both local (R_l) and nonlocal (R_{nl}) resistance in the absence of magnetic field is generally considered as a direct proof of a 2D TI state. In that case the current flows through a sample along its borders and resistance exists regardless of the positions of the voltage probes with respect to current contacts, either in the

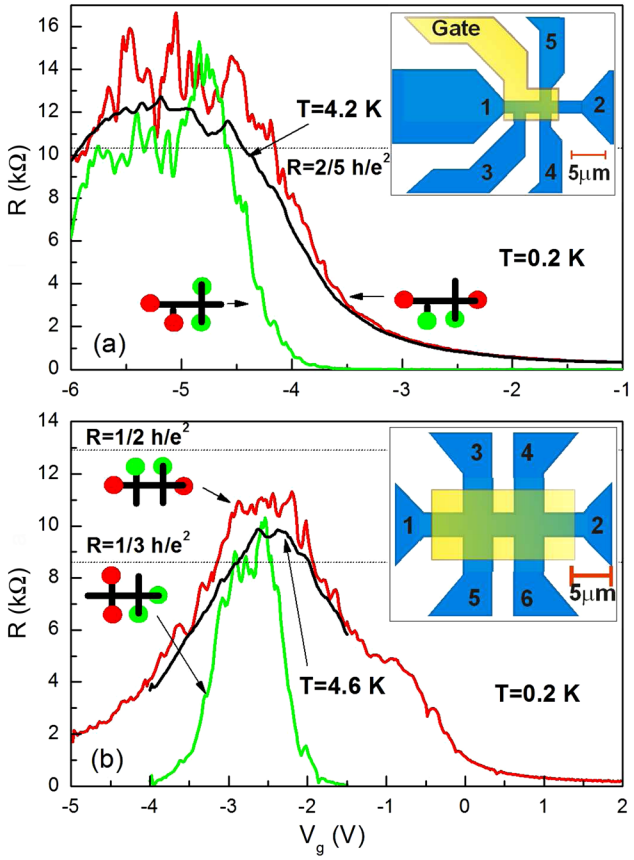

FIG. 3 (color online). $R(V_g)$ dependences for local (red curves) and nonlocal (green curves or a lighter shade of grey) resistance measurement configurations obtained in two different types of microscopic samples. The samples layouts are shown schematically in the insets. All curves were obtained at 0.2 K except the black curves measured at temperatures 4.2 and 4.6 K. Opposite to each curve the corresponding measurement configuration is shown schematically. The dashed horizontal lines mark the resistance values expected for these configurations in the case of a purely ballistic transport via edge current states.

ballistic [21] or diffusive [22] regime. Figures 2(a) and 2(b) show R_l and R_{nl} as functions of the gate voltage for various temperatures in the range 0.2–3.3 K and Fig. 2(c) shows these resistances as functions of temperature for the gate voltages corresponding to the maxima of local and nonlocal resistance, i.e., when the Fermi level is in the middle of the insulating gap. Qualitatively, the behavior of local and nonlocal resistances is similar. When the temperature is above 1 K, both resistances grow exponentially with decreasing temperature. For lower temperatures the resistance growth slows down and for $T < 0.5$ K it obeys a power law $R \propto T^{-\alpha}$ ($\alpha \approx 0.5$). As this takes place, even though at higher temperatures, the local resistance is several orders of magnitude greater than the nonlocal one; at $T < 1$ K the nonlocal resistance becomes larger. The described behavior of R_l and R_{nl} is typical for the 2D TI, as it follows from the fundamental difference in the relative contributions of the bulk and edge transport when measuring them in local and nonlocal configurations [22]. At higher temperatures, when the bulk contribution is still sufficiently large, R_{nl} is exponentially small compared to the sheet resistivity. With decreasing T the bulk contribution to transport also decreases, and at some T, depending on the insulating bulk gap, becomes negligibly small. Under these conditions the difference in the resistance values measured in local and nonlocal configurations is determined only by the distribution of currents flowing along the sample perimeter and by the position of the voltage probes. At $T < 0.5$ K for all investigated configurations the resistance at its maximum is more than an order of magnitude greater than $h/2e^2$, which means that the transport via the edge states is diffusive.

Let us discuss in more detail the temperature dependence of R_{nl} and R_l. First, the maximum of the curves $R_{nl}(V_g)$ and $R_l(V_g)$ shifts to the right with the temperature decreasing. Such behavior was not observed in 2D TI previously and is probably related to the complicated energy spectrum of the system investigated, or, more specifically, to its much smaller gap that is further diminished by the bulk bands density of states tails. Second, as has already been mentioned, with lowering temperature the resistance, after the exponential growth, continues to increase, but at a much lower rate, following a power law $R \propto T^{0.5}$, typical for quasi-1D wires in a weak localization regime. We have attempted a quantitative description of the temperature dependence of the local and nonlocal resistance peak values by using the model proposed in [10,16]. The activation energy for the bulk transport has been chosen as a fitting parameter. The results of the calculation presented in Fig. 2(c) show a reasonable agreement between the calculated and measured dependences. The value of the activation energy found from fitting the calculation to experiment is approximately 1.2 meV for local and nonlocal configurations alike, as was expected. This value is less than $\Delta = 3.3$ meV, the indirect insulating gap value obtained from the energy spectrum calculation. This discrepancy is not surprising if one considers the disorder due to impurities and QW thickness fluctuations that are always present in a real HgTe sample. In such a case one may expect that the activation energy would correspond to the mobility gap rather than to a much larger calculated insulating bulk gap [24].

The mean free path for the edge states transport determined experimentally for the diffusive transport in the macroscopic samples is 2–5 μm for sample I and 12–14 μm for sample II (See Supplemental Material [10]). On this account our QWs look promising for observation of ballistic transport via edge states, considering that in the majority of the previously studied 2D TI this value was close to 1 μm. For this purpose, two types of microscopic samples were fabricated, one with the dimensions $W = 1.7$ and $L = 1.8$ μm [see inset to Fig. 3(a)] and the other an H-shaped bridge with the width $W = 3.2$ μm and the length $L = 2.8$ μm [see inset to Fig. 3(b)].

Figure 3 shows the dependence of the local (red) and nonlocal (green) resistance versus gate voltage measured in the two microscopic samples. When the bias applied to the gate decreases below −1 V [Fig. 3(a)] [2 V in Fig. 3(b)], the local resistance starts to grow gradually as the Fermi level first descends to the bottom of the conduction band and then enters the insulating bulk gap at $V_g \approx -4.5$ V [Fig. 3(a)] [$V_g \approx -2$ V in Fig. 3(b)]. The nonlocal response is close to zero when the Fermi level remains in the conduction band. The abrupt increase in the nonlocal resistance as the Fermi level enters the insulating gap signals, as well as in the macroscopic case, the presence of the edge current states in the gap. The calculation of the local and nonlocal resistance values expected in our microstructures in the case of ballistic transport via edge states is quite simple and is indicated by the dashed lines for each configuration shown in Fig. 3. As may be seen, the average resistance values measured at $T = 0.2$ K in the gate voltage range corresponding to the Fermi level staying in the insulating gap are quite close to the levels expected for purely ballistic transport. With the negative bias increasing, the Fermi level enters the valence band and the sample resistance decreases. Relying on this data, it is possible to conclude that our microstructures demonstrate a quasiballistic edge transport in a 2D TI. This fact is quite important considering that up until now the observations of ballistic transport in HgTe-based 2D TI reported in [19] has remained unique. We also observe other similarities with the results reported in [19]. In particular, when the Fermi level lies in the insulating gap there are random fluctuations both in the local and nonlocal resistance. The amplitude of these fluctuations sharply decreases as the temperature increases, indicating their mesoscopic origin.

Figure 3 also shows the variation of the local resistance with temperatures in the range from 0.2 to 4.2 K in our microstructures. One can see that this variation is noticeably weaker than in our macroscopic samples [compare with Fig. 2(c)]. This fact has a simple explanation. In microstructures the sheet conductance due to the bulk transport is the same as in macroscopic samples, while the resistance to transport via edge states decreases by approximately 1 order of magnitude. This observation also indicates that the mean free path for the edge states transport in our QWs must be comparable to, or higher than, ≈ 10 μm. We also observe a suppression of both local and nonlocal quasiballistic conductance by weak magnetic field, a behavior typical for the 2D TI state [19,25], which will be reported elsewhere.

We believe that our observation of relatively high mean free path for the edge states is not accidental but rather related to the advantages associated with the use of a wider quantum well. Indeed, the width of any QW is not uniform but fluctuates from point to point around its average value d with the amplitude δ. That δ is determined by the growth technology employed and is practically independent of the QW width. The fluctuation of the QW width results in a random potential in the bulk of the QW. However, the amplitude of that random potential would be much smaller in a wider QW as it is proportional to $1/(d^3)$. From that point of view it is clear that a wider QW well is more advantageous for the observation of ballistic transport in 2D TI.

The results of the present study confirm that the 2D TI state in HgTe QWs is quite robust and exists in a sizeable range of well widths despite of the fact that the energy spectrum in such QWs is complicated and strongly dependent on the well width.

The work was supported by the RFBI Grant No. N15-02-00217-a, by the RAS Grant No. 24.11 and by FAPESP, CNPq (Brazilian agencies).

[1] M. Z. Hasan and C. L. Kane, Rev. Mod. Phys. **82**, 3045 (2010);X-L. Qi and S.-C. Zhang, Rev. Mod. Phys. **83**, 1057 (2011).
[2] X.-L. Qi and S.-C. Zhang, Phys. Today **63**, 33 (2010).
[3] J. E. Moore and L. Balents, Phys. Rev. B **75**, 121306(R) (2007).
[4] J. E. Moore, Nature (London) **464**, 194 (2010).
[5] C. L. Kane and E. J. Mele, Phys. Rev. Lett. **95**, 146802 (2005).
[6] H. Zhang and S.-C. Zhang, Phys. Status Solidi RRL **7**, 72 (2013).
[7] C.-X. Liu, H. J. Zhang, B. Yan, X.-L. Qi, T. Frauenheim, X. Dai, Z. Fang, and S.-C. Zhang, Phys. Rev. B **81**, 041307 (2010).
[8] H.-Z. Lu, W.-Yu. Shan, W. Yao, Q. Niu, and S.-Q. Shen, Phys. Rev. B **81**, 115407 (2010).
[9] L. Wu, M. Brahlek, R. V. Aguilar, A. V. Stier, C. M. Morris, Y. Lubashevsky, L. S. Bilbro, N. Bansal, S. Oh, and N. P. Armitage, Nat. Phys. **9**, 410 (2013).
[10] See Supplemental Material at http://link.aps.org/supplemental/10.1103/PhysRevLett.114.126802, which includes Refs. [22,11–17], for details on the Kane model parameters, sample description, the bulk + edge model, and magnetoresistance measurements.
[11] Z. D. Kvon, E. B. Olshanetsky, E. G. Novik, D. A. Kozlov, N. N. Mikhailov, I. O. Parm, and S. A. Dvoretsky, Phys. Rev. B **83**, 193304 (2011).
[12] J. Maciejko, C. X. Liu, Y. Oreg, X. L. Qi, C. Wu, and S. C. Zhang, Phys. Rev. Lett. **102**, 256803 (2009).
[13] A. Ström, H. Johannesson, and G. I. Japaridze, Phys. Rev. Lett. **104**, 256804 (2010).
[14] J. I. Vayrynen, M. Goldstein, and L. I. Glazman, Phys. Rev. Lett. **110**, 216402 (2013).
[15] D. A. Abanin, K. S. Novoselov, U. Zeitler, P. A. Lee, A. K. Geim, and L. S. Levitov, Phys. Rev. Lett. **98**, 196806 (2007).
[16] G. M. Gusev, E. B. Olshanetsky, Z. D. Kvon, A. D. Levin, N. N. Mikhailov, and S. A. Dvoretsky, Phys. Rev. Lett. **108**, 226804 (2012).

[17] V. T. Dolgopolov, G. V. Kravchenko, and A. A. Shashkin, Solid State Commun. **78**, 999 (1991).
[18] B. A. Bernevig, T. L. Hughes, and S. C. Zhang, Science **314**, 1757 (2006).
[19] M. König, S. Wiedmann, C. Brune, A. Roth, H. Buhmann, L. W. Molenkamp, X.-L. Qi, and S.-C. Zhang, Science **318**, 766 (2007).
[20] O. E. Raichev, Phys. Rev. B **85**, 045310 (2012).
[21] A. Roth, C. Brüne, H. Buhmann, L. W. Molenkamp, J. Maciejko, X.-L. Qi, and S.-C. Zhang, Science **325**, 294 (2009).
[22] G. M. Gusev, Z. D. Kvon, O. A. Shegai, N. N. Mikhailov, S. A. Dvoretsky, and J. C. Portal, Phys. Rev. B **84**, 121302 (R) (2011).
[23] Z. D. Kvon, E. B. Olshanetsky, D. A. Kozlov, E. G. Novik, N. N. Mikhailov, and S. A. Dvoretsky, Low Temp. Phys. **37**, 202 (2011).
[24] *The Quantum Hall Effect*, edited by R. E. Prange and S. M. Girvin (Springer-Verlag, New York, 1987).
[25] G. M. Gusev, E. B. Olshanetsky, Z. D. Kvon, N. N. Mikhailov, and S. A. Dvoretsky, Phys. Rev. B **87**, 081311(R) (2013).